Asymptotic normalization coefficients from the ^{14}C$(d,p)^{15}$C reaction

A. M. Mukhamedzhanov,[1] V. Burjan,[2] M. Gulino,[3] Z. Hons,[2] V. Kroha,[2] M. McCleskey,[1] J. Mrázek,[2] N. Nguyen,[4] F. M. Nunes,[4] Š. Piskoř,[2] S. Romano,[3] M. L. Sergi,[3] C. Spitaleri,[3] and R. E. Tribble[1]
[1]*Cyclotron Institute, Texas A&M University, College Station, Texas 77843, USA*
[2]*Nuclear Physics Institute, Czech Academy of Sciences, CZ-250 68 Řež near Prague, Czech Republic*
[3]*Università di Catania and INFN Laboratori Nazionali del Sud, Catania, Italy*
[4]*National Superconducting Cyclotron Laboratory and Department of Physics and Astronomy, Michigan State University, East Lansing, Michigan 48824, USA*
(Received 26 March 2011; revised manuscript received 30 June 2011; published 29 August 2011)

The ^{14}C$(n,\gamma)^{15}$C reaction plays an important role in inhomogeneous big bang models. In Timofeyuk *et al.* [Phys. Rev. Lett. **96**, 162501 (2006)] it was shown that the ^{14}C$(n,\gamma)^{15}$C radiative capture at astrophysically relevant energies is a peripheral reaction, i.e., the overall normalization of its cross section is determined by the asymptotic normalization coefficient (ANC) for ^{15}C $\rightarrow$ ^{14}C $+ n$. Here we present new measurements of the ^{14}C$(d,p)^{15}$C differential cross sections at deuteron incident energy of 17.06 MeV and the analysis to determine the ANCs for neutron removal from the ground and first excited states of ^{15}C. The results are compared with previous estimations.

DOI: 10.1103/PhysRevC.84.024616 PACS number(s): 25.45.−z, 24.50.+g, 21.10.Jx, 25.40.Lw

I. INTRODUCTION

In inhomogeneous big bang models [1–3] the ^{14}C$(n,\gamma)^{15}$C reaction plays an important role, being the part of the chain ^{7}Li$(n,\gamma)^{8}$Li$(\alpha,n)^{11}$B$(n,\gamma)^{12}$B$(\beta^-)^{12}$C$(n,\gamma)^{13}$C$(n,\gamma)^{14}$C$(n,\gamma)^{15}$C. Due to the high neutron abundance, the ^{14}C$(n,\gamma)^{15}$C reaction can compete strongly with the other reactions on ^{14}C, which all lead to the production of heavier nuclei ($A > 20$). In [4] it was shown that the ^{14}C$(n,\gamma)^{15}$C radiative capture at astrophysically relevant energies is a peripheral reaction, i.e., the overall normalization of its cross section is determined by the asymptotic normalization coefficient (ANC) for ^{15}C $\rightarrow$ ^{14}C $+ n$. This ANC has been determined in [4] using the mirror symmetry from the width of the broad resonance state in ^{15}F. The recommended value is $C^2_{0\,1/2} = 1.89 \pm 0.11$ fm^{-1}. Here $l = 0$ and $j = 1/2$ are the orbital angular momentum and total angular momentum of the neutron in ^{15}C. This result was obtained using the resonance width of the broad state in ^{15}F experimentally measured in [5]. However, the value of the width of a broad resonance significantly depends on the method used to extract it [6]. Hence the uncertainty of the ANC determined from the mirror symmetry can be large. Joint analysis of the ^{15}C(g.s.) knockout data from [7] and [8] carried in [9] lead to $C^2_{0\,1/2} = 1.48 \pm 0.18$ fm^{-1}. In [10] the ANC $C^2_{0\,1/2} = 1.64 \pm 0.03$ fm^{-1} was determined from the analysis of the Coulomb dissociation of ^{15}C on ^{208}Pb at 68 MeV/nucleon [11]. The calculated cross section for the direct radiative capture ^{14}C$(n,\gamma)^{15}$C using this ANC is in excellent agreement with the latest direct measurements [12]. Excellent agreement of the analysis done in [10] with measurements of [12] allow us to conclude that the ANC determined in [10,13] can be referred to as a recommended value.

To check the consistency of the ANC for the neutron removal from ^{15}C, other types of reactions can be used. In [14] the analysis of the ^{14}C$(d,p)^{15}$C experimental data [15] obtained at 14-MeV deuteron energy was carried out testing different approaches to the reaction theory:

(1) Distorted wave Born approximation (DWBA) using the global Perey and Perey optical potential for the deuteron [16];

(2) DWBA using a deuteron potential which fits the d − ^{14}C elastic scattering;

(3) Adiabatic distorted wave approximation (ADWA) where the deuteron potential is constructed as the sum of the proton and neutron optical potentials taken at half of the deuteron energy [17] with finite range correction as in [18].

This last method takes into account deuteron breakup explicitly. The CH89 parametrization [19] was used for all nucleon potentials (including the exit channel). The single-particle radius for the neutron bound state potential was varied in the interval 1.01−1.91 fm. For choice (1) the obtained interval for the extracted $C^2_{01/2}$ was 2.516−2.777 fm^{-1}; for choice (2) the obtained interval of $C^2_{01/2}$ was 2.60−2.71 fm^{-1}. For choice (3) a significant reduction was observed with the interval of the extracted $C^2_{01/2}$: 2.08−2.44 fm^{-1}. However, this reduction was not enough to reconcile the ANC extracted from the (d,p) reaction with the values determined from breakup reactions and (n,γ) processes, which are significantly lower [10,13]. Higher order transfer couplings were found to have a significant effect on the reduction of the ANC [14]. For example, for choice (2) at $r_0 = 1.3$ fm, the extracted ANC drops by 26% [14], reaching $C^2_{01/2} = 2.14$ fm^{-1}, which coincides with the value obtained from the ADWA analysis for this geometry. However, even such a drop is not enough to reconcile the ANCs obtained from different sources. Multistep excitations within the coupled channel Born approximation (CCBA) were shown to be too weak in ^{14}C$(d,p)^{15}$C due to the small B(E2) connecting the first excited state in ^{14}C [14]. Despite all the various reaction theories explored in [14], it appears impossible to reconcile the ANC extracted from transfer (d,p) with that from direct radiative capture [12], mirror symmetry [4], or Coulomb dissociation [10]. Indeed, the lowest of the square of the ANC from transfer from [14] is about 30% higher than the value dictated by radiative capture and the analysis of Coulomb dissociation [10]. Is this disagreement an indication that the various reaction models tested in [14] are not adequate for loosely bound exotic nuclei like ^{15}C, or could it be that the overall normalization of the cross section in [15] is not correct? Since the ^{14}C$(d,p)^{15}$C reaction measurements presented in [15] were done 35 years ago, new, more accurate measurements of this reaction, in the context described above, are highly desirable.

With the aim of exploring the consistency of the ANC obtained from different reactions, we present here new and improved measurements of the angular distributions of ^{14}C$(d,p)^{15}$C for a deuteron incident energy of 17.06 MeV.

In [15] the minimal reported angle for the transition to the ground state of ^{15}C was smaller than 10°, with a systematic uncertainty in the overall normalization of the measured cross section of 20%. Since the ANC is determined by normalizing the calculated differential cross section to the experimental cross section at the main (stripping) peak of the angular distribution (in the case under consideration it is zero degrees), it is important to take data for small scattering angles. In this work we decreased the minimal angle to 6.6° with the systematic uncertainty about 10%. In addition, we used the recently implemented finite-range adiabatic model (FR-ADWA) [20] to extract the ANCs for neutron transfer to the ground and first excited states of ^{15}C, therefore taking into account the most important higher-order effect in this reaction—deuteron breakup. In addition, deuteron elastic scattering was measured in a wide angular range and is presented in the Appendix.

II. EXPERIMENTAL ARRANGEMENT

Measurement of the differential cross sections of the ^{14}C$(d,p)^{15}$C reaction was carried out on the U-120M isochronous cyclotron at the Nuclear Physics Institute of the Czech Academy of Sciences. The experiment was realized with a momentum-analyzed 17.06-MeV deuteron beam impinged on the self-supporting ^{14}C target. At this energy we are able to obtain the optimal deuteron beam with the highest intensity and best energy resolution. The best quality of the beam is especially important in the case under consideration due to the necessity of identifying all impurities in the ^{14}C target.

Reaction products were detected by four $\Delta E - E$ telescopes consisting of 250–400 μm and 4-mm-thick Si(Li) detectors, correspondingly. Telescopes were provided with collimators 2×3 mm^2. Their distances from the target center were 160 mm. One telescope was fixed at 15 degrees as a monitor of target and the remaining three were movable between laboratory angles of 6–67 degrees for the angular distribution measurements. Thickness of the ^{14}C target was checked by scanning using α-source as well as by reaction products in different output reaction channels. Thickness of the target was also controlled by measurement on the Mylar target of known stoichiometry and thickness 146 μg/cm^2. Each exposition of the ^{14}C target was followed by exposition of the Mylar target at the same angle. The pure ^{14}C contents in target was 175 μg/cm^2 with 40 μg/cm^2 of admixtures. The integrated charge of beam was measured with uncertainty less then 3%. The total uncertainties due to the target thickness, detector solid angle, charge collection, and the statistical ones were less than 10% in the forward angles of the angular distributions. The differential cross sections were obtained for deuteron elastic scattering and for two proton groups corresponding to population of the ground state $1/2^+$ and the 0.740-MeV state $5/2^+$ in ^{15}C. A typical spectrum is shown in Fig. 1. Experimental angular distributions were measured at a 6°–75° angular range in the laboratory system.

III. REACTION THEORY AND NUMERICAL DETAILS

For many years, the standard DWBA was the main tool for studying deuteron stripping reactions. In the standard DWBA, the one-step transfer matrix element is evaluated with incoming and outgoing distorted waves calculated by respectively fitting the deuteron and proton elastic scattering with local optical potentials. The transition operator contains finite range effects as well as the full complex remnant term. The main idea of DWBA is that the transition matrix element is small enough that one can use first-order perturbation theory. In many cases, this approximation does not hold (i.e., [14]). Since the nuclear potential is quite large by itself ($\sim$100 MeV), the smallness of the transition operator can be fulfilled only if the reaction is peripheral enough, so that the matrix element from the transition operator becomes small. The pioneering work by Johnson and Sopper [17] clearly demonstrated the deficiency of the standard DWBA and developed the ADWA model, which starts from a three-body approach and is not perturbative. The original ADWA [17] introduced the zero-range approximation for the deuteron, but recently studies using FR-ADWA have shown that finite-range effects can be significant [20]. One important advantage of the FR-ADWA used here to analyze the transfer data is that only nucleon optical potentials are required; the CH89 parametrization [19] is used in this work. To check the impact of the ambiguity of the optical potentials on extracted ANCs, we also performed calculations with Koning and Delaroche (KD) optical potentials [21]. For the sake of comparison we also present results obtained within the standard DWBA. For the deuteron bound state, the Reid soft core potential [22] is used as in [20]. Calculations of the deuteron adiabatic potentials are performed within TWOFNR [23] and the transfer calculations are performed with FRESCO [24].

A. Results

Experimental angular distributions of protons from the reaction ^{14}C$(d,\,p)^{15}$C populating the ground state $2s_{1/2}$ and the first excited $1d_{5/2}$ state ($E_x = 0.740$ MeV) in ^{15}C are shown in Figs. 2 and 3, respectively. The calculations using FR-ADWA with the CH89 optical potential angular distributions for the transitions to the ground state and first excited states reproduce the experimental data in the vicinity of the first peak, which is sufficient to determine an ANC (Sec. III B). Note that calculations with the KD optical potentials generate angular distributions practically identical with the CH89 angular

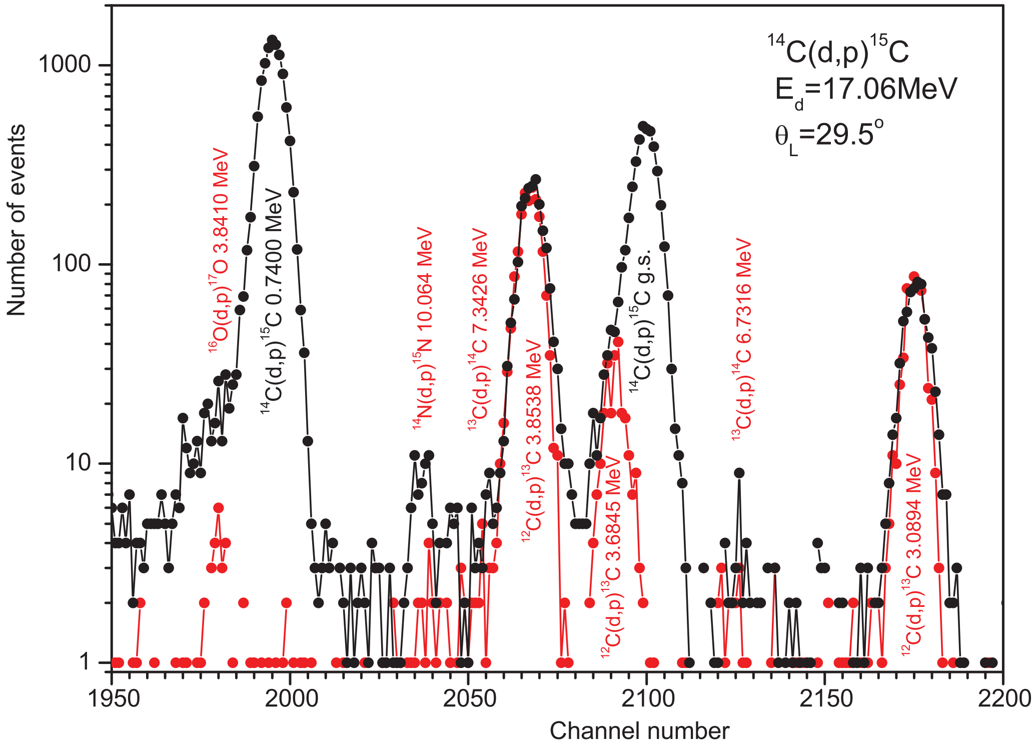

FIG. 1. (Color online) Spectrum of protons from the ^{14}C$(d,p)^{15}$C reaction at $\theta_{\rm lab} = 29.5^o$. The proton groups from the ^{14}C target, including admixtures are shown by a black line. The normalized proton groups from the Mylar target shown by red color indicate contamination of used ^{14}C target as described in the text. All admixtures are marked by description in red letters.

distributions. That is why in Figs. 2 and 3 only angular distributions obtained with CH89 potentials are shown. To compare with FR-ADWA, in Fig. 2 we also present the cross sections obtained within the standard DWBA using four different combinations of the optical potentials: D1-P1, D1-P2, D2-P1, and D2-P2 (see Tables II and III in Appendix). Within DWBA, the angular distributions for either transition to the ground or first excited state in ^{15}C are best described by the combination of optical model potentials D1-P2, although all other combinations describe equally well the first peak. These

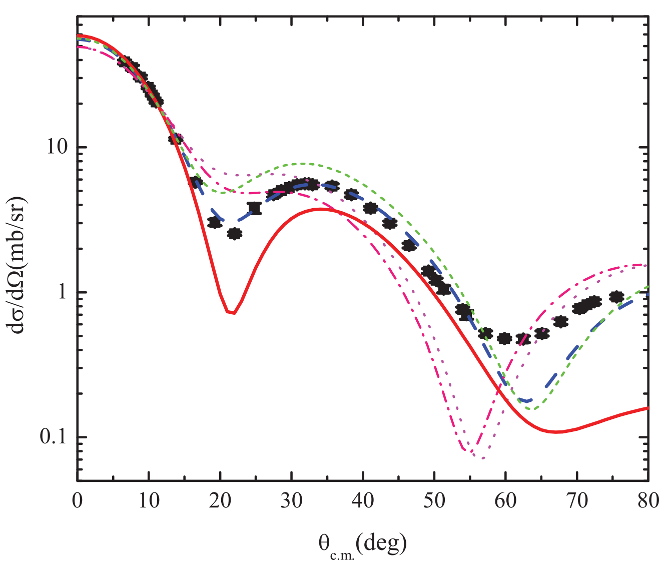

FIG. 2. (Color online) Angular distributions from the ^{14}C$(d,p)^{15}$C reaction for the transitions leading to the ground state $2s_{1/2}$ in ^{15}C: FR-ADWA with CH89 potentials, red thick solid line; D1-P1, pink dashed-dotted line; D1-P2, blue thick dashed line; D2-P1, magenta dotted line; D2-P2, green short-dashed line.

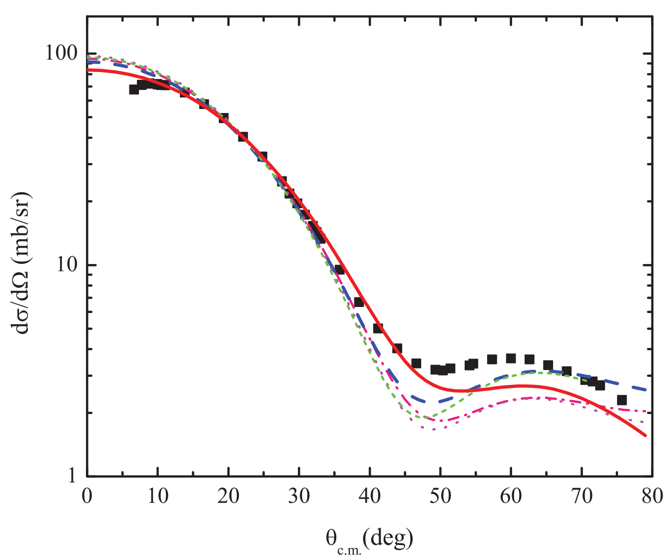

FIG. 3. (Color online) Angular distributions from the ^{14}C$(d,p)^{15}$C reaction for the transitions leading to the first excited state $1d_{5/2}$ in ^{15}C. Notations are the same as in Fig 2.

potentials do produce large differences in the normalization of the cross section, which obviously has implications for the extracted ANC (Sec. III B). One could argue that the FR-ADWA does not reproduce the data at angles beyond the first stripping peak, while there does exist a combination of deuteron and proton potentials within the DWBA approach that is better at reproducing the data. We do not consider this a valid argument because one cannot use the same data set to fit optical potentials and extract a reliable normalization. In addition, note that the cross section at the first minimum is 20 times smaller then at the first peak. The disagreement between the experimental data and FR-ADWA near the first minimum is very typical and is usually due to reaction mechanisms excluded from the model space, where contributions become more pronounced at larger angles. These contributions are small compared to the large stripping at the forward peak. Note that the calculated angular distribution for the transition to the first excited state is also well reproduced in the vicinity of the first peak, except for a small drop at very small angles, which all theoretical curves do not describe. This feature cannot be reproduced by adjusting interactions.

B. Asymptotic normalization coefficients

For extracting the ANC, it is the angular range around the main stripping maximum that is most important. The ANC is simply determined from the normalization of the calculated differential cross section to the experimental angular distribution. However, for the method to work, one must first ensure the reaction is peripheral. In order to check peripherality of the ^{14}C$(d,p)^{15}$C reaction we have repeated FR-ADWA calculations with CH89 potentials cutting the interior. A cutoff radius of 3 fm is used to estimate the error in the peripheral approximation. We found an 11% effect for the transition to the ground state and a 4% effect for the transition to the excited state. Since the ^{14}C$(d,p)^{15}$C reaction is mostly peripheral, the overall normalization of its differential cross section is determined by the square of the product of the ANC for the neutron removal from ^{15}C and the ANC for the deuteron wave function. Taking into account that the ANC for the deuteron wave function is known (for the Reid soft core potential [22] it is $C_{np} = 0.88$ fm$^{-1/2}$), the ^{15}C ANC can be readily extracted. Table I contains the ANCs obtained. In order to check the uncertainty of the determined ANCs to the ambiguity of the optical potentials, we have performed FR-ADWA calculations with two different sets of global optical potentials, CH89 and KD. In Table I we present the square of the ANC values obtained from FR-ADWA for CH89 and KD potentials separately with the uncertainties coming from a 10% experimental systematic uncertainty and 11% uncertainty for the transition to the ground state (4% for the transition to the first excited state) due to the small nonperipherality of the reaction. Since these uncertainties are added in quadrature, the total uncertainty for the square of the ANCs obtained for each potential set is 15% for the transition to the ground state and 11% for the transition to the excited state. We also find mean values of the ANCs generated by CH89 and KD potentials with 7% (6%) standard deviation for the square of the ANC for the ground state (excited state). We assign the total uncertainty of 16% for the square of the ANC for the ground state and 12% for the first excited state. The total assigned uncertainty to the square of the ANC is obtained by adding in quadrature the uncertainty due to the ambiguity of the optical potentials, systematic experimental uncertainty, and error of the peripheral approximation.

TABLE I. ANCs from the ^{14}C$(d,\,p)^{15}$C reaction.

State	Method	C^2_{lj} (fm^{-1})
$s_{1/2}$	FR-ADWA	
	CH89	1.72 ± 0.26
	KD	1.56 ± 0.23
	Mean value	1.64 ± 0.26
	DWBA	
	D1-P1	1.62
	D1-P2	1.94
	D2-P1	1.80
	D2-P2	2.32
	Mean value	1.92 ± 0.46
$d_{5/2}$	FR-ADWA	
	CH89	$(3.70 \pm 0.41)\ 10^{-3}$
	KD	$(3.40 \pm 0.37)\ 10^{-3}$
	Mean value	$(3.55 \pm 0.43)\ 10^{-3}$
	DWBA	
	D1-P1	0.0035
	D1-P2	0.0034
	D2-P1	0.0038
	D2-P2	0.0037
	Mean value	$(3.6 \pm 0.8)\ 10^{-3}$

Our result for $C^2_{0\,1/2} = 1.64 \pm 0.26$ fm^{-1} agrees very well with the result obtained in [10] and with the value dictated by the direct radiative capture [12]. It also overlaps with the value obtained from the mirror symmetry [4], but it is lower than the ANC determined in [14] from the analysis of the ^{14}C$(d,\,p)^{15}$C reaction at 14-MeV deuteron energy. This significant difference can be due to the inconsistencies in the absolute normalization of the measured cross sections. To compare our ANC with the one determined from the analysis of the ^{14}C$(d,\,p)^{15}$C reaction at 14-MeV deuteron energy [14], we should consider only ADWA with CH89 optical potentials, i.e., with the same potentials which were used in [14]. The average square of the ANC obtained in [14] within ADWA with CH89 optical potentials and with approximate finite-range corrections, for nine different sets of the neutron bound state potentials, is $C^2_{0\,1/2} = 2.19 \pm 0.10$ fm^{-1}, which is 27% higher than our value $C^2_{0\,1/2} = 1.72 \pm 0.26$ fm^{-1}. In order to check this possibility, we have repeated the calculations at 14 MeV within FR-ADWA using the CH89 optical potentials. The ratio of the experimental differential cross sections measured by us and in [15] at 10° is 2.16, while the theoretical ratio is 1.67. We conclude that the absolute value of the differential cross section in [15] is overestimated by $2.16/1.67 = 1.293$. By dividing the square of the ANC obtained in [14] by 1.293 we get a significantly lower value $C^2_{0\,1/2} = 1.69$ fm^{-1}, which agrees well with the value $C^2_{0\,1/2} = 1.72 \pm 0.26$ fm^{-1} obtained from

TABLE II. Parameters of the optical model fit in the input channel $d + {}^{14}$C.

Pot	V (MeV)	r (fm)	a (fm)	W (MeV)	r_w (fm)	a_w (fm)	W_d (MeV)	r_d (fm)	a_d (fm)	r_c (fm)
Seed Cole[a]	125.4	0.81	1.07	–	–	–	17.4	1.93	0.36	0.81
D1[b]	130.44	0.81	0.8471	–	–	–	11.74	1.8953	0.4183	0.81
Seed Perey[c]	82.8	1.0	1.092	–	–	–	6.99	1.935	0.485	1.3
D2[d]	98.27	1.0	0.8969	–	–	–	14.18	1.7862	0.4335	1.3

[a]Seed Cole: parameters from [26].
[b]D1: fit of our elastic scattering data.
[c]Seed Perey: parameter set from [16].
[d]D2: fit of our elastic scattering data.

the present analysis with CH89 optical potentials at 17 MeV (see Table I).

Going back to the 17.06-MeV deuteron energy, if one were to use DWBA in the analysis, one would have to take into account the uncertainty associated with the optical potentials under the constraint of deuteron elastic scattering. From Table I one can conclude that the extracted ANCs significantly depend on the choice of the optical potentials. From the range of the obtained ANCs we determine the error coming from the ambiguity of the deuteron and proton optical potentials in the DWBA calculation: 18.2%. However, in addition, one must consider the contribution from the interior and the experimental error. Summing these errors in quadrature, the total error in the square of the ANC for the ground state extracted using DWBA becomes 24% and for transition to the first excited state 22%. This produces $C^2_{0\,1/2} = 1.92 \pm 0.46$ fm^{-1} and $C^2_{2\,5/2} = (3.6 \pm 0.8) \times 10^{-3}$ fm^{-1}, with significantly larger uncertainties than for FR-ADWA. Even though the mean value obtained for $C^2_{0\,1/2}$ within DWBA is larger than that obtained within FR-ADWA, the methods agree within errors.

IV. SUMMARY AND CONCLUSION

We have presented a study of the reaction ^{14}C$(d,p)^{15}$C at the deuteron incident energy of 17.06 MeV populating the ground and the first excited states of ^{15}C. The analysis shows that the stripping to the ground state and to the first excited state of ^{15}C is almost peripheral, allowing us to determine the ANCs for the neutron removal from the ground and first excited states of ^{15}C. Both ANCs show a weak dependence on the geometry of the neutron bound state potential in ^{15}C. Using the FR-ADWA with two different sets of the optical parameters, we determined $C^2_{0\,1/2} = 1.64 \pm 0.26$ fm^{-1} and $C^2_{2\,5/2} = (3.55 \pm 0.43) \times 10^{-3}$ fm^{-1}. Our analysis finds that the older measurements from [15] overestimated the cross section at forward angles by ∼29%, and the correct renormalization of these data provides an ANC closer to our extracted values. For comparison, we also performed the standard DWBA analysis with four sets of the optical potentials, constrained by elastic deuteron scattering at the same energy. The obtained ANC is higher than the value extracted with FR-ADWA and, most importantly, with larger error bars. One of the main conclusions of our study is that the ^{14}C$(d,p)^{15}$C reaction can be used as a tool to determine the ANCs, but to obtain reliability and better accuracy it is important to go beyond DWBA.

ACKNOWLEDGMENTS

This work was supported by the Grant No. LC07050 of the Czech MSMT, Grant No. M10480902 of the Czech Academy, GACR Grant No. P203/10/310, Grant No. LH11001 of the AMVIS Project, the US Department of Energy under Grants No. DE-FG02-93ER40773, No. DE-FG52-06NA26207, No. DE-FG52-08NA28552, No. DE-SC0004958, and No. DE-SC0004087 (topical collaboration TORUS), and the National Science Foundation under Grants No. PHY-0852653 and No. PHY-0800026.

APPENDIX: OPTICAL MODEL POTENTIALS IN THE CONVENTIONAL DWBA

We have measured the angular distribution of the elastic scattering of deuterons on ^{14}C, and for its analysis we use the phenomenological optical potential in the general

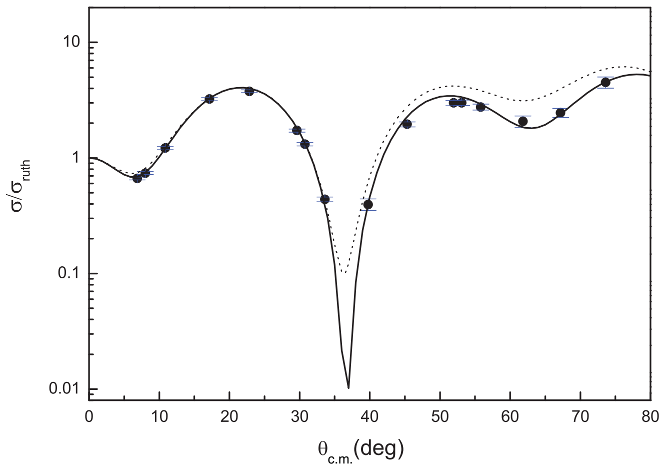

FIG. 4. (Color online) The angular distribution of the deuteron elastic scattering on ^{14}C obtained with the beam energy of 17.06 MeV. Curves represent final fits generated by optical potential sets D1 (dashed line) and D2 (solid line) given in Table II.

TABLE III. Optical model parameters in the output channel $p + {}^{15}\text{C}$.

Pot	V (MeV)	r (fm)	a (fm)	W_d (MeV)	r_d (fm)	a_d (fm)	W_{so} (MeV)	r_{so} (fm)	a_{so} (fm)	r_c (fm)	Ref.
P1	63	1.13	0.65	9.7	1.13	0.51	7.5	1.13	0.65	1.25	[27]
P2	53.3	1.11	0.64	7.14	1.40	0.36	5.68	0.983	0.34	1.25	[16]

Woods-Saxon form:

$$U(r) = V_c(r) - Vf(x_o) + \left(\frac{\hbar}{m_\pi c}\right)^2 V_{so}(\sigma l)\frac{1}{r}\frac{d}{dr}f(x_{so}) - i\left[Wf(x_w) - 4W_d\frac{d}{dr}f(x_d)\right], \quad \text{(A1)}$$

where $f(x_i) = (1 + e^{x_i})^{-1}$ and $x_i = (r - r_i A^{1/3})/a_i$ represents the usual Woods-Saxon form factor. V, W, W_d, and V_{so} are the real, imaginary volume, imaginary surface, and spin-orbital potential depths, respectively, with appropriate radii r_i and diffusiveness a_i, and $V_c(r)$ is the Coulomb potential of a uniformly charged spherical nucleus of a radius $r_{\text{coul}} = r_c A^{1/3}$.

The computer code ECIS79 [25] was used for the search of optical model parameters in the input channel. We looked for the parameters which describe best the angular distribution of the elastic scattering of deuterons on the ^{14}C nucleus at energy 17.06 MeV. We have taken two sets of the optical model parameters as seed parameters used to describe the elastic scattering on the ^{14}C nucleus. We did not use seed potentials with spin-orbit coupling. The first seed set, which we found in literature, was used by Cole *et al.* [26] for the calculation of the deuteron elastic scattering on ^{14}C at deuteron energy of 10 MeV. The second most suitable seed set describes the deuteron elastic scattering on the neighboring nucleus ^{14}N at 21-MeV energy [16]. The advantage of this data set is a more realistic deuteron Coulomb radius ($r_c = 1.3$ fm) of the optical model than in the case of Cole seed data ($r_c = 0.81$ fm). When fitting the optical model parameters (V, a, W_d, r_d, a_d) we minimized the χ^2 function using the uncertainties of the elastic-scattering differential cross section. Resulting optical model parameters from both seed sets are given in Table II and denoted as D1 (fit of Cole seed data [26]) and D2 (fit of seed data taken from Perey and Perey [16]). The stability of fits was checked by changing input seed data by 10% only to convince ourselves that the same resulting optical model parameters were obtained. Final fits are shown in Fig. 4, where the calculated angular distributions of deuterons using D1 and D2 optical potentials are compared with the experimental one. The optical model parameter set D2 gives better agreement with experimental data. Optical model parameters used for the output channel are given in Table III. They were taken from Curtis et al. [27] and from Perey and Perey [16] and described angular distributions of the proton elastic scattering on ^{14}C and ^{14}N, respectively, because the elastic-scattering data for the ^{15}C nucleus were not available at the relevant energy.

[1] J. Applegate and C. Hogan, Phys. Rev. D **31**, 3037 (1985).
[2] J. Applegate, C. Hogan, and R. Scherrer, Astrophysical J. **329**, 527 (1988).
[3] R. Malaney and W. Fowler, Ap. J. **333**, 14 (1988).
[4] N. K. Timofeyuk, D. Baye, P. Descouvemont, R. Kamouni, and I. J. Thompson, Phys. Rev. Lett. **96**, 162501 (2006).
[5] V. Z. Goldberg, G. G. Chubarian, G. Tabacaru, L. Trache, R. E. Tribble, A. Aprahamian, G. V. Rogachev, B. B. Skorodumov, and X. D. Tang, Phys. Rev. C **69**, 031302(R) (2004).
[6] A. M. Mukhamedzhanov, B. F. Irgaziev, V. Z. Goldberg, Y. V. Orlov, and I. Qazi, Phys. Rev. C **81**, 054314 (2010).
[7] E. Sauvan *et al.*, Phys. Rev. C **69**, 044603 (2004).
[8] V. Maddalena *et al.*, Nucl. Phys. A **682**, 332 (2001).
[9] Texas A&M Progress Report 20012002, p. 16.
[10] N. C. Summers and F. M. Nunes, Phys. Rev. C **78**, 011601(R) (2008).
[11] T. Nakamura *et al.*, Nucl. Phys. A **722**, 301c (2003).
[12] R. Reifarth *et al.*, Phys. Rev. C **77**, 015804 (2008).
[13] H. Esbensen, Phys. Rev. C **80**, 024608 (2009).
[14] D. Y. Pang, F. M. Nunes, and A. M. Mukhamedzhanov, Phys. Rev. C **75**, 024601 (2007).
[15] J. D. Goss, P. L. Jolivette, C. P. Browne, S. E. Darden, H. R. Weller, and R. A. Blue, Phys. Rev. C **12**, 1730 (1975).
[16] C. M. Perey and F. G. Perey, At. Data Nucl. Data Tables **17**, 1 (1976).
[17] R. C. Johnson and P. J. R. Soper, Phys. Rev. C **1**, 055807 (1970).
[18] G. L. Wales and R. C. Johnson, Nucl. Phys. A **274**, 168 (1976).
[19] R. L. Varner, W. J. Thompson, T. L. McAbee, E. J. Ludwig, and T. B. Clegg, Phys. Rep. **201**, 57 (1991).
[20] N. B. Nguyen, F. M. Nunes, and R. C. Johnson, Phys. Rev. C **82**, 014611 (2010).
[21] A. J. Koning and J. P. Delaroche, Nucl. Phys. A **713**, 231 (2003).
[22] V. Reid, Ann. Phys. (NY) **50**, 411 (1968).
[23] M. Igarashi *et al.*, Computer program TWOFNR, University of Surrey version, 2008.
[24] I. J. Thompson, Comput. Phys. Rep. **7**, 167 (1988).
[25] J. Raynal, Code ECIS79 (unpublished).
[26] W. S. Cole, T. Mo, H. R. Weller, and J. J. Ramirez, Nucl. Phys. A **213**, 107 (1973).
[27] T. H. Curtis, H. F. Lutz, D. W. Heikkinen, and W. Bartolini, Nucl. Phys. A **165**, 19 (1971).